Pergamon

Int. J. Heat Mass Transfer. Vol. 39, No. 11, pp. 2319–2327, 1996

0017-9310/96 $15.00+0.00

0017-9310(95)00312-6

The influence of sorption isotherms on the drying of porous materials

A. J. J. VAN DER ZANDEN and A. M. E. SCHOENMAKERS

Laboratory of Separation Technology, Eindhoven University of Technology, P.O. Box 513, 5600 MB Eindhoven, The Netherlands

(*Received* 7 *April* 1995 *and in final form* 1 *August* 1995)

Abstract—A model is presented for the simultaneous vapour and liquid transport in porous materials. The model describes the evaporation inside a porous material with a mass transfer coefficient and a specific evaporating surface. The model also includes the effect of sorption isotherms. Predictions of the model are compared with experimental results found in the literature. Copyright © 1996 Elsevier Science Ltd.

1. INTRODUCTION

The process of moisture transport in porous materials is not fully understood yet. The problem is tried to be solved in different ways. Network models are popular; for instance Nowicki *et al.* [1], or diffusion models, see refs. [2–5]. Also some measurements can be found in the literature, for instance Schoenherr and Mocikat [6]. The diffusion approach was also followed by van der Zanden *et al.* [7]. They gave a model for the diffusion coefficient of liquid in porous materials. The prediction of this model was modified by van der Zanden [8].

The interaction between the liquid and vapour phase inside a partially saturated porous material was modelled by van der Zanden *et al.* [9] and by van der Zanden [10]. They described the evaporation inside a porous material with a mass transfer coefficient and a specific evaporating surface. The main discrepancy with the experiments was that their model predicted a receding liquid front inside a porous material, while the experiments did not show such a characteristic behaviour. They explained this difference by the neglect of the sorption isotherm in their model.

The purpose of this paper is to extend the theory of van der Zanden *et al.* [9, 10] to include the sorption isotherm in the model (Section 2). In Sections 3 and 4 the approach will be outlined to obtain the numerical solution of the model. In Section 5 the model will be tested with the experimental results of Ketelaars [11] who measured moisture profiles in clay during drying. Two clays which he used in his study will be used in this paper namely (in his terminology) clay A and clay C.

2. MOISTURE TRANSPORT IN POROUS MATERIALS

A sample of a porous material is considered which has a volume V. This sample can contain an amount of liquid water having a volume V_l. The volume fraction water is then V_l/V. The concentration of liquid water, C_l, in kg per m^3 sample is

$$C_l = \rho \frac{V_l}{V}, \tag{1}$$

where ρ is the density of liquid water. In a porous material there exists an equilibrium between C_l and the water activity in the vapour phase, a_w, the sorption isotherm. The concentration water vapour in air when the air is saturated is denoted by $c_{v,sat}$, where a small c is used in contrast with a capital C to indicate that it is based on a smaller volume, the volume of the vapour phase. The vapour concentration in the vapour phase in equilibrium with C_l is $a_w c_{v,sat}$. The water vapour concentration in the pores need not be in equilibrium with C_l. For instance in Fig. 1 the bulk concentration vapour, c_v, at position B can be smaller than the equilibrium concentration at the evaporating surface S, $a_w c_{v,sat}$. The result is a water vapour flux, J, from the surface S to the bulk which can be modelled with a mass transfer coefficient k_m

$$J = k_m(a_w c_{v,sat} - c_v). \tag{2}$$

The specific evaporating surface in the porous material where the water evaporates from is denoted α and is supposed to be independent of liquid concentration. The specific rate of evaporation, G, then follows from equation (2)

$$G = k_m \alpha (a_w c_{v,sat} - c_v). \tag{3}$$

The volume fraction of the vapour phase is

$$\varepsilon - \frac{V_l}{V} \tag{4}$$

in which ε is the porosity. With expression (4) the concentration of water in vapour form in the porous sample is

NOMENCLATURE

a_w	water activity [−]	V	volume [m^3]
a	adjustment factor in the grid [−]	x	position [m].
c	concentration in the vapour phase [kg m^{-3}]	Greek symbols	
C	concentration in the porous material [kg m^{-3}]	α	specific evaporating surface [m^2 m^{-3}]
D	diffusion coefficient	ε	porosity
G	specific rate of evaporation [kg m^{-3} s^{-1}]	ξ	logarithmic position [−]
H	height of the sample [m]	ρ	density of water [kg m^{-3}].
J	vapour flux [kg m^{-2} s^{-1}]	Indices	
k_m	mass transfer coefficient [m s^{-1}]	f	largest filled pore
n	effective flux in the pores [kg m^{-2} s^{-1}]	l	liquid
N	moisture flux [kg m^{-2} s^{-1}]	o	overall (liquid plus vapour)
R	radius [m]	out	leaving the sample
t	time [s]	sat	saturation
		v	vapour.

$$C_v = \left(\varepsilon - \frac{V_l}{V}\right)c_v = \left(\varepsilon - \frac{C_l}{\rho}\right)c_v. \tag{5}$$

Now the differential equation describing the liquid transport inside the porous material is

$$\frac{\partial C_l}{\partial t} = \frac{\partial}{\partial x}\left[D_l \frac{\partial C_l}{\partial x}\right] - k_m \alpha (a_w c_{v,sat} - c_v) \tag{6}$$

where D_l is the diffusion coefficient which depends on the liquid concentration C_l. The differential equation for the vapour transport can be derived by considering the effective vapour flux in the pores

$$n = -D_v \frac{\partial c_v}{\partial x} \tag{7}$$

in which D_v is the effective diffusion coefficient of water vapour, which is supposed to be independent of concentration and concentration gradient. With the arguments leading to equation (5) the effective flux in the porous material is then

$$N = \left(\varepsilon - \frac{C_l}{\rho}\right)n \tag{8}$$

which with equation (7) is

$$N = -D_v\left(\varepsilon - \frac{C_l}{\rho}\right)\frac{\partial c_v}{\partial x}. \tag{9}$$

A vapour balance over a slice of porous material, as illustrated in Fig. 2, is

$$N_x\,dt + G\,dx\,dt - N_{x+dx}\,dt = dx\,dC_v \tag{10}$$

which leads to

$$\frac{\partial C_v}{\partial t} = D_v\left(\varepsilon - \frac{C_l}{\rho}\right)\frac{\partial^2 c_v}{\partial x^2} - \frac{D_v}{\rho}\frac{\partial c_v}{\partial x}\frac{\partial C_l}{\partial x} + G, \tag{11}$$

or

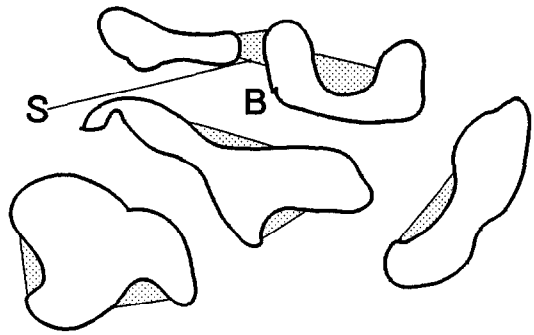

Fig. 1. Schematic representation of a partially saturated porous material.

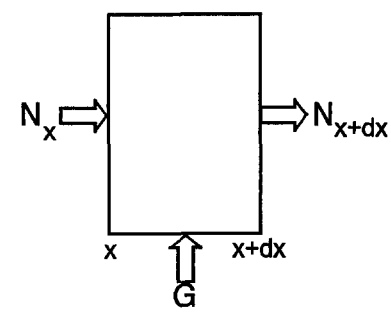

Fig. 2. Mass balance to derive the differential equation describing the vapour concentration.

$$\frac{\partial c_v}{\partial t}\left(\varepsilon-\frac{C_l}{\rho}\right)-\frac{c_v}{\rho}\frac{\partial C_l}{\partial t}=D_v\left(\varepsilon-\frac{C_l}{\rho}\right)\frac{\partial^2 c_v}{\partial x^2}$$

$$-\frac{D_v}{\rho}\frac{\partial c_v}{\partial x}\frac{\partial C_l}{\partial x}+k_m\alpha(a_w c_{c,sat}-c_v). \quad (12)$$

3. PARAMETERS

In the previous section a model has been proposed to describe the transport of moisture through porous materials. In this study this model will be used in the case of water transport through clays which were studied by Ketelaars [11]. A few parameters are used in the model. These parameters of clays A and C were examined extensively by van der Zanden *et al.* [9].

They reported the porosity for clays A and C as 0.40 and 0.30, respectively. The diffusion coefficient of the liquid, D_l, was fitted with the results of Ketelaars and for clay A was given as

$$D_l = 1.7804\cdot 10^{-9}\exp\left(0.01272C_l-\frac{145.59}{C_l+51.47}\right) \quad (13)$$

and for clay C as

$$D_l=\frac{0.02508}{R_f}(R_f^2-1.6\cdot 10^{-17}) \quad (14)$$

in which R_f is the radius of the largest filled pores, given by

$$R_f = 4\cdot 10^{-9}\exp(0.0149C_l). \quad (15)$$

The parameters k_m and α never appear separately, but always as a product. Van der Zanden *et al.* [9] argued that $k_m\alpha$ has a minimal value of the order $10^5\ s^{-1}$.

The effective diffusion coefficient of water in the vapour phase, D_v, was reported to be $2.13\cdot 10^{-6}\ m^2\ s^{-1}$ in clay A and $2.54\cdot 10^{-6}\ m^2\ s^{-1}$ in clay C.

In addition to these parameters the equilibrium between C_l and the water activity in the vapour, a_w, was measured by Ketelaars [11] and is given in Fig. 3 for clay A and clay C. Clay C is much more hygroscopic than clay A.

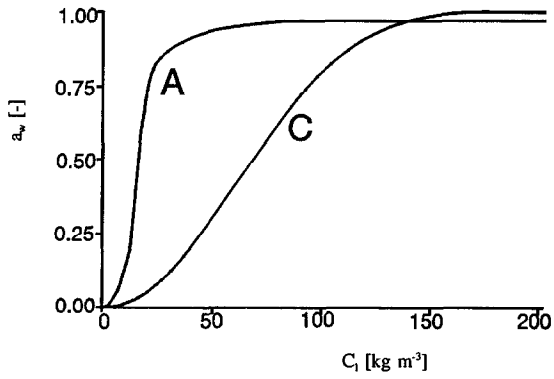

Fig. 3. Sorption isotherms of clay A and C. The water activity is given as a function of the liquid concentration.

4. NUMERICAL SOLUTION

In Section 2 differential equations (6) and (12) were derived. To make the mathematical problem complete the boundary conditions at the drying surface ($x = 0$) and the isolated surface ($x = H$) must also be given. Clearly no flux occurs at the isolated surface and the boundary conditions are

$$\frac{\partial c_v}{\partial x}=0 \quad \text{at } x=H \quad (16)$$

and

$$\frac{\partial C_l}{\partial x}=0 \quad \text{at } x=H. \quad (17)$$

As also stated by van der Zanden *et al.* [9], the boundary condition at the drying surface is not so clear. At the drying surface a flux occurs out of the drying clay, N_{out}. This flux is the sum of the vapour flux and the liquid flux

$$N_{out}=D_v\left(\varepsilon-\frac{C_l}{\rho}\right)\frac{\partial c_v}{\partial x}+D_l\frac{\partial C_l}{\partial x} \quad \text{at } x=0. \quad (18)$$

If the drying surface is very wet the liquid flux dominates over the vapour flux. However, if the drying surface is very dry, the vapour flux dominates over the liquid flux. During the drying process the vapour flux becomes more significant and the liquid flux becomes less significant. More study concerning the physics at the drying surface is needed to describe properly what happens at this surface. If the vapour concentration, c_v, is in equilibrium with the liquid concentration, C_l, except maybe in a small interval very close to the drying surface, the moisture profiles inside the clay are not so much influenced by whether the flux at the surface is formed by a vapour flux or by a liquid flux. This is illustrated in Fig. 4 which depicts one moisture profile inside a clay sample and a small interval Δx where the liquid profile is not in equilibrium with the vapour profile in the sample. The moisture which is going out of the clay sample can follow path 1 (the liquid flux) or it can follow path 2 (evaporation very close to the surface and then out of the sample in the form of vapour). Whether path 1 or 2 (or a combination of the two) is followed hardly

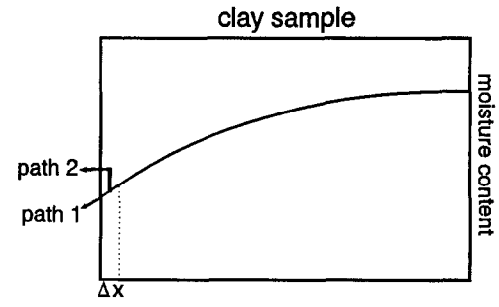

Fig. 4. The moisture in the sample can leave the sample following one of two paths with the difference that evaporation takes place whether inside or outside the sample.

influences the moisture profile outside the small interval Δx. For now the flux is thought of as being formed by a vapour flux

$$N_{out} = D_v\left(\varepsilon - \frac{C_l}{\rho}\right)\frac{\partial c_v}{\partial x} \quad \text{at } x = 0 \tag{19}$$

and the liquid flux must then be zero

$$0 = D_l\frac{\partial C_l}{\partial x} \quad \text{at } x = 0. \tag{20}$$

In the numerical simulations a mesh is needed which is fine at the drying surface. In the Appendix a reasoning is presented with the result that a coordination transformation from x to ξ is used given by

$$\xi = \frac{\ln\left(x\frac{a^{ng}-1}{H}+1\right)}{\ln(a)} \tag{21}$$

in which ng is the number of gridpoints minus 1 and H is the height of the clay sample. The factor a can be adjusted to get a finer or coarser grid at the drying surface. In this study ng is 300 and a is 1.02. When using this new coordinate the differential equations (6) and (12) become, respectively,

$$\frac{\partial C_l}{\partial t} = \left(\frac{a^{ng}-1}{Ha^{\xi}\ln(a)}\right)^2\left[\frac{\partial C_l}{\partial \xi}\left(\frac{\partial D_l}{\partial \xi} - D_l\ln(a)\right) + D_l\frac{\partial^2 C_l}{\partial \xi^2}\right] - k_m\alpha(a_w c_{v,sat} - c_v) \tag{22}$$

and

$$\frac{\partial c_v}{\partial t}\left(\varepsilon - \frac{C_l}{\rho}\right) - \frac{c_v}{\rho}\frac{\partial C_l}{\partial t} = D_v\left(\frac{a^{ng}-1}{Ha^{\xi}\ln(a)}\right)^2 \times \left(\varepsilon - \frac{C_l}{\rho}\right)\left[\frac{\partial^2 c_v}{\partial \xi^2} - \ln(a)\frac{\partial c_v}{\partial \xi}\right] - \frac{D_v}{\rho}\left(\frac{a^{ng}-1}{Ha^{\xi}\ln(a)}\right)^2\frac{\partial c_v}{\partial \xi}\frac{\partial C_l}{\partial \xi} + k_m\alpha(a_w c_{v,sat} - c_v). \tag{23}$$

This coordinate ξ is very easy to use in the computations because the gridpoints have the ξ-values $0, 1, 2, \ldots, ng-1, ng$. The boundary conditions become

$$\frac{\partial c_v}{\partial \xi} = 0 \quad \text{at } \xi = ng, \tag{24}$$

$$\frac{\partial C_l}{\partial \xi} = 0 \quad \text{at } \xi = ng, \tag{25}$$

$$N_{out} = \frac{D_v(a^{ng}-1)}{H\ln(a)a^{\xi}}\left(\varepsilon - \frac{C_l}{\rho}\right)\frac{\partial c_v}{\partial \xi} \quad \text{at } \xi = 0 \tag{26}$$

and

$$0 = \frac{\partial C_l}{\partial \xi} \quad \text{at } \xi = 0. \tag{27}$$

The equations (22) and (23) are solved numerically by the Crank–Nicolson method using the simplification that the process of vapour diffusion is quasi-steady according to the reasoning as given by van der Zanden *et al.* [9]. The term on the left side of equation (23) then becomes zero.

The moisture content at the drying surface cannot become smaller than zero. If during a simulation such a situation were to occur, the boundary condition (26) is replaced by the boundary condition

$$c_v = 0 \quad \text{at } \xi = 0 \tag{28}$$

and is then maintained during the rest of that simulation.

5. RESULTS

For the two clays used in this study moisture profiles were experimentally obtained by Ketelaars [11] by using a scanning neutron radiography technique. The total moisture content of a sample is, in this paper, obtained by integrating these moisture profiles. Differentiating the moisture content with respect to time gives the flux, N_{out}, at the drying surface.

The water vapour concentration in the pores, $c_{v,sat}$, is computed with the Antoine relation and the ideal gas law.

Van der Zanden *et al.* [9] reported some doubts whether Ketelaars started the drying process with a uniform moisture content. To circumvent any errors attributed to this problem, in this study all computations will use the first profile measured by Ketelaars as the initial condition.

The height of the drying samples of clay A and C were reported by Ketelaars to be for both 0.0295 m.

In this study more attention is given to clay C than to clay A because clay C is more hygroscopic and the influence of the sorption isotherm may be expected to be somewhat larger than in clay A.

In Fig. 5 the computed profiles in clay C are presented for the value of $k_m\alpha$ 10^5 s^{-1} after 3692 (initial condition), 21362, 37552 and 55212 s. A value of $k_m\alpha$ equal to 10^8 s^{-1} gave almost identical results. In the moisture content C_v is neglected with respect to C_l. Since the moisture profiles are not sensitive to the values of the parameter $k_m\alpha$ in the rest of this study the value 10^5 s^{-1} will be used.

The influence of including the sorption isotherm in the model is studied in Fig. 6 in which two almost coinciding profiles are plotted, one as a result of a computation including the sorption isotherm and the other without sorption isotherm, both at $t = 4284$ s being the time at which a receding liquid front will start to occur in the case where the sorption isotherm is neglected. The difference between the profiles on $t = 4284$ s is not clearly visible in Fig. 6. In Fig. 7 the ξ-scale is used to plot both profiles. In this figure the difference is clearly visible, it also shows that the profile computed with the model without sorption isotherm goes to zero and the other profile does not. The

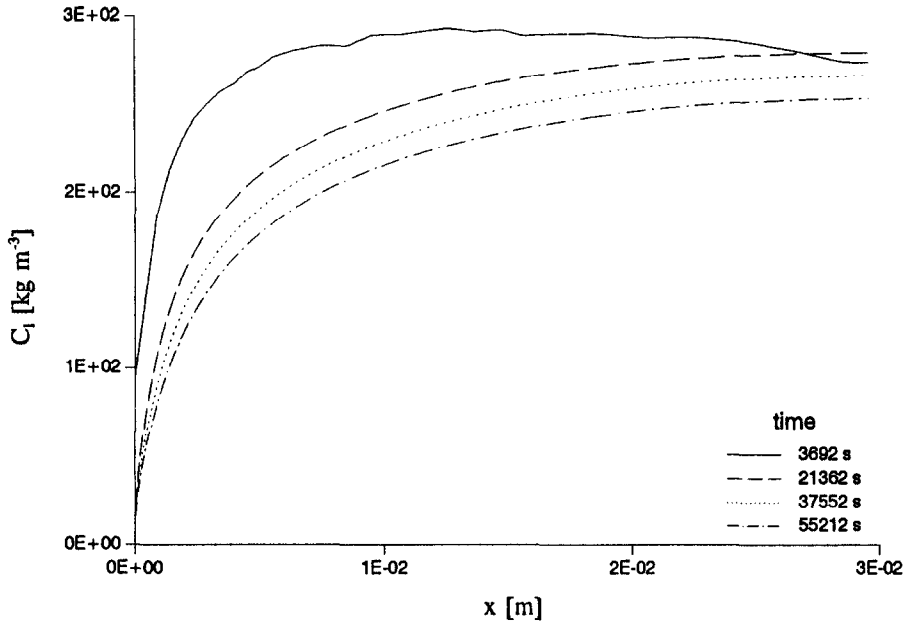

Fig. 5. Computed moisture profiles in clay C with the parameter time and a $k_m\alpha$-value of 10^5 s^{-1}.

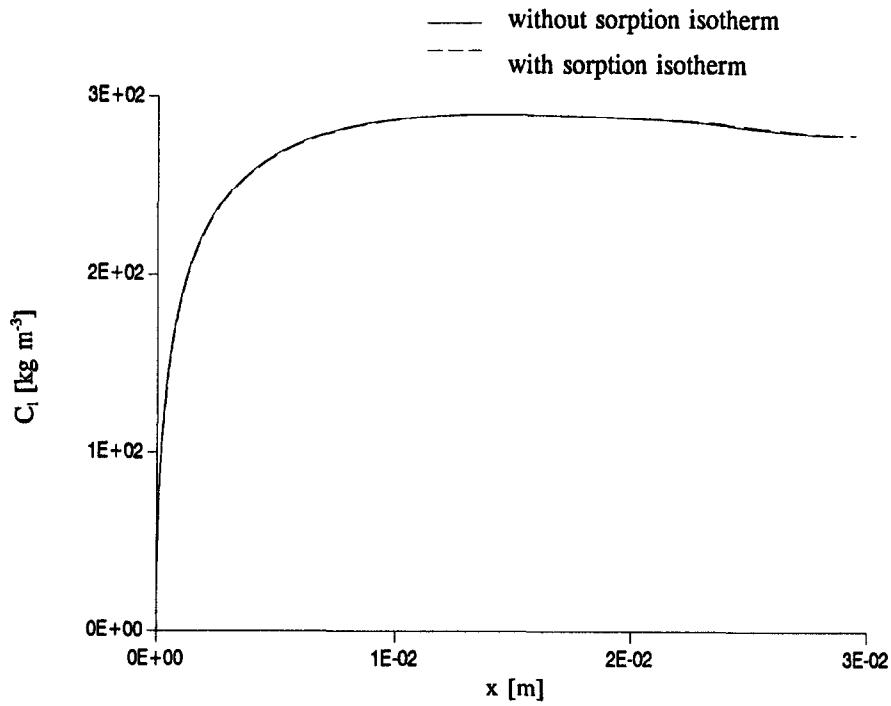

Fig. 6. Two moisture profiles, one with the model including sorption isotherm and the other without.

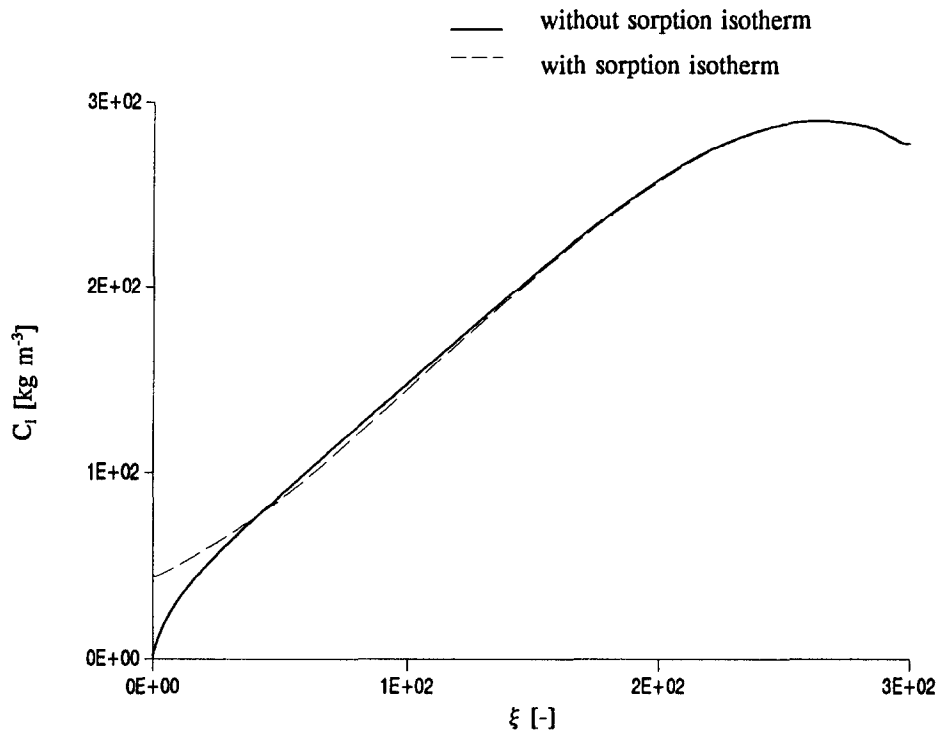

Fig. 7. The profiles of Fig. 6 now using the ξ-scale.

case where the sorption isotherm was neglected was examined by van der Zanden *et al.* [9, 10] and they reported the computed liquid front receding into the clay sample.

In Fig. 8 the computed profiles (solid lines) of clay C are compared with the profiles as measured by Ketelaars (symbols). The computed profiles are seen not to agree with the experimentally obtained profiles. At

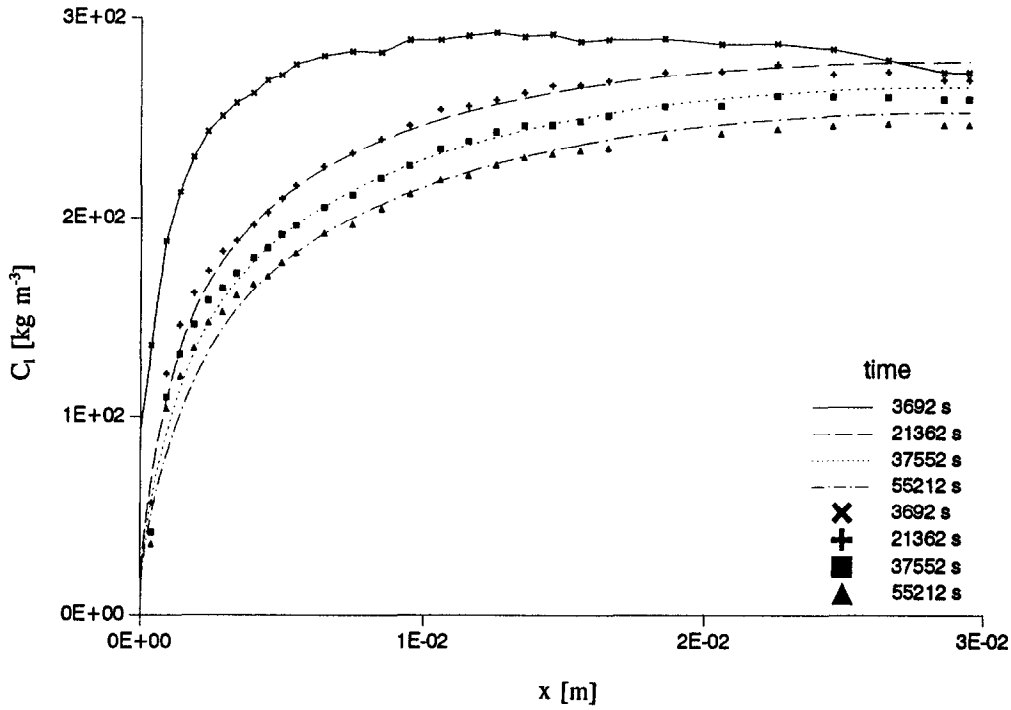

Fig. 8. Comparison of prediction of the model for moisture profiles (lines) with the measurements of Ketelaars [11] (symbols) for clay C.

the drying surface the measured profiles are steeper than the computed profiles. This can be caused by a too large D_l in the computations. Van der Zanden *et al.* [7, 9, 10] interpreted the diffusion coefficient, as measured by Ketelaars, to be equal to D_l. This assumption may be wrong in the case where the sorption isotherm may not be neglected. The sum of the vapour and liquid flux inside a porous material is written with an overall diffusion coefficient, D_o, as

$$D_o\left(\frac{\partial C_l}{\partial x}+\frac{\partial c_v}{\partial x}\right)=D_v\left(\varepsilon-\frac{C_l}{\rho}\right)\frac{\partial c_v}{\partial x}+D_l\frac{\partial C_l}{\partial x}. \tag{29}$$

Now let it be assumed that the concentration in the vapour phase is in equilibrium with the concentration in the liquid phase

$$c_v = c_{v,sat}a_w. \tag{30}$$

The derivative of equation (30) substituted in equation (29) gives, if the gradient of C_v is neglected with respect to the gradient of C_l,

$$D_o\frac{\partial C_l}{\partial x}=D_v\left(\varepsilon-\frac{C_l}{\rho}\right)c_{v,sat}\frac{\partial a_w}{\partial C_l}\frac{\partial C_l}{\partial x}+D_l\frac{\partial C_l}{\partial x}, \tag{31}$$

or

$$D_l = D_o - D_v\left(\varepsilon-\frac{C_l}{\rho}\right)c_{v,sat}\frac{\partial a_w}{\partial C_l}. \tag{32}$$

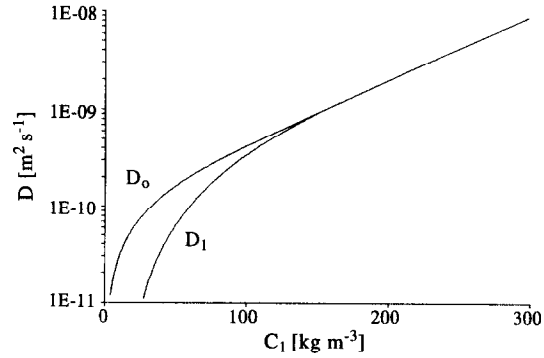

Fig. 9. Overall diffusion coefficient, D_o, and the diffusion coefficient of the liquid, D_l, as a function of moisture content, C_l.

Now if the diffusion coefficient as measured by Ketelaars is assumed to be the overall diffusion coefficient, D_o, equation (32) can be used to calculate the diffusion coefficient of the liquid, D_l. In Fig. 9 D_o and D_l are plotted as a function of moisture content for clay C. Using this new value for D_l in the computations result in the profiles as shown in Fig. 10 (lines), together with profiles as measured by Ketelaars (symbols). Now the agreement is much better than in Fig. 8.

For clay A the computed profiles are shown in Fig. 11 (lines) together with the measured profiles (symbols). The agreement is not very good. This can-

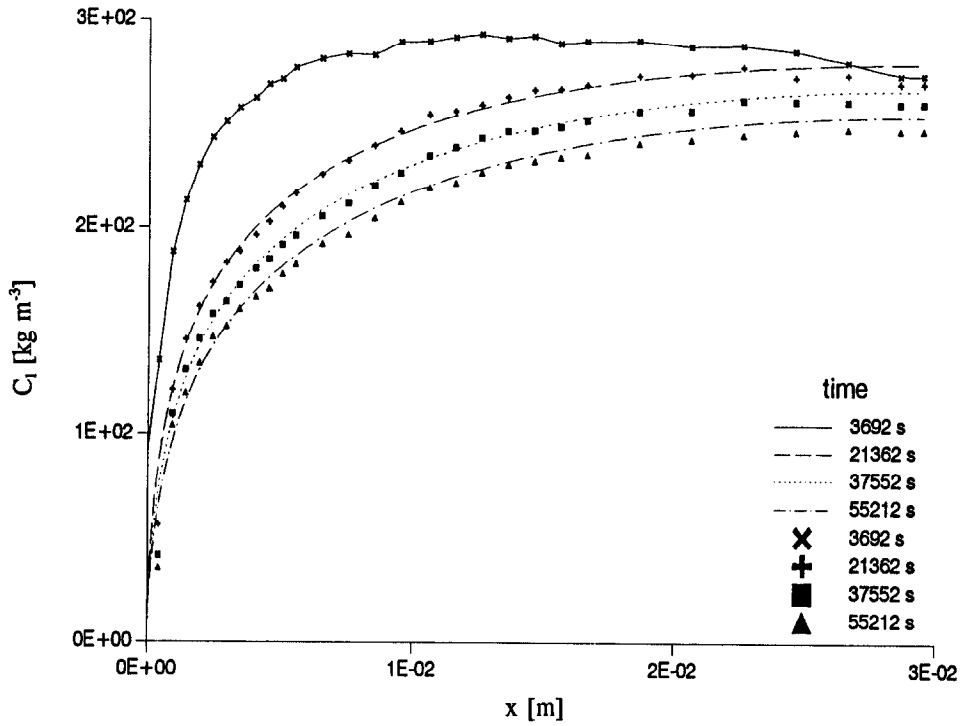

Fig. 10. Comparison of the prediction of the model for moisture profiles (lines) with the measurements of Ketelaars [11] (symbols) for clay C, now using the modified diffusion coefficient of the liquid.

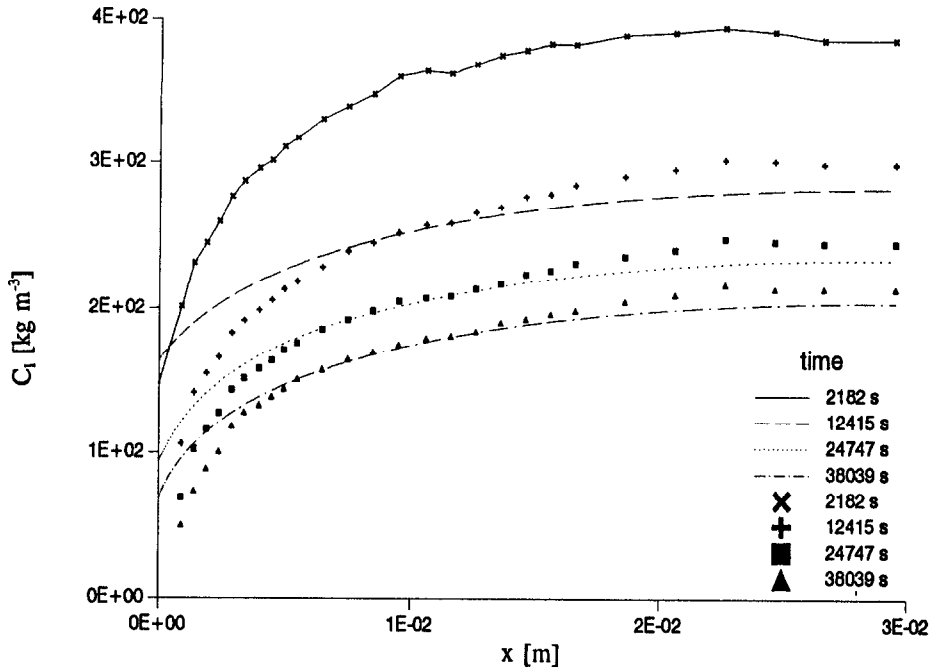

Fig. 11. Comparison of the prediction of the model for moisture profiles (lines) with the measurements of Ketelaars [11] (symbols) for clay A.

not be caused by the neglect of the sorption isotherm because the sorption isotherm starts to deviate significantly from $a_w = 1$ at $C_l = 50\,\mathrm{kg\,m^{-3}}$, being a value which is not reached in the simulations. Ketelaars extracted the diffusion coefficient from the profiles, while in this study the profiles are computed using the diffusion coefficient. Clearly there is no reconciliation between these two studies concerning this part.

6. CONCLUSION AND DISCUSSION

A model has been presented that describes the moisture transport in porous materials including the effect of the sorption isotherm. In the model the parameter combination $k_m\alpha$ describes the evaporation inside the porous material. Within the physical realistic range this parameter combination does not have a large influence on the moisture profiles indicating that, except maybe very close to the evaporating surface the concentration in the vapour phase is in equilibrium with the concentration in the liquid phase. Using this notion the model clarifies how an overall diffusion coefficient, which includes transport in the liquid phase and in the vapour phase, is formed by the diffusion coefficient of mass in liquid form and by the diffusion coefficient of mass in vapour form. The assumption of van der Zanden *et al.* [7] that in clay C the transport of water is formed only by liquid water transport has been proved not to be valid for small moisture contents.

This paper describes the interaction between the liquid and vapour phase inside a porous material. A full understanding of the problem of moisture transport needs a better understanding of the process of diffusion in the liquid and vapour phase, i.e. D_l and D_v. Further knowledge of what happens at the drying surface would complete the understanding of the whole process.

REFERENCES

1. S. C. Nowicki, H. T. Davis and L. E. Scriven, Microscopic determination of transport parameters in drying porous media, *Drying Technol.* **10**, 925–946 (1992).
2. W. Blumberg and E.-U. Schluender, Simultaneous vapor and liquid diffusion in partially wetted porous media, *Drying Technol.* **11**, 41–64 (1993).
3. S. Chen and S. Whitaker, Moisture distribution during constant rate drying period for unconsolidated porous media: failure of the diffusion theory, *Proceedings of the International Drying Symp.*, Boston, pp. 39–48 (1986).
4. J. R. Puiggali, M. Quintard and S. Whitaker, Drying granular porous media: gravitational effects in the isenthalpic regime and the role of diffusion models, *Drying Technol.* **6**, 601–629 (1988).
5. S. Whitaker and W. T. H. Chou, Drying of granular porous media—theory and experiment, *Drying Technol.* **1**, 3–33 (1983).
6. M. Schoenherr and H. Mocikat, Capillary porous media: internal heat and mass transport, *Drying Technol.* **9**, 139–158 (1991).
7. A. J. J. van der Zanden, W. J. Coumans, P. J. A. M. Kerkhof and A. M. E. Schoenmakers, Isothermal moisture transport in partially saturated porous media, *Drying Technol.* **14** (7–8) (1996).
8. A. J. J. van der Zanden, A possible revision of the results of a model for moisture transport in partially saturated porous media, *Drying Technol.* **13**, 2227–2231 (1995).
9. A. J. J. van der Zanden, A. M. E. Schoenmakers and P. J. A. M. Kerkhof, Isothermal vapour and liquid transport inside clay during drying, *Drying Technol.* **14** (3) (1996).
10. A. J. J. van der Zanden, Modelling and simulating sim-

ultaneous liquid and vapour transport in partially saturated porous materials. In *Mathematical Modelling and Numerical Techniques in Drying Technology* (Edited by A.S. Mujumdar and I.W. Turner). Marcel Dekker, New York (1996).
11. A. A. J. Ketelaars, Drying deformable media: kinetics, shrinkage and stresses, Ph.D. Thesis, University of Eindhoven, The Netherlands (1992).

APPENDIX

In the computations a grid must be used which is fine at the drying surface and coarse further in the sample. To deduce the mathematical relation between the Cartesian position coordinate x and the coordinate ξ as used in the text, a grid is used which has meshes which are a factor a smaller than its larger neighbour, as is depicted in Fig. A1. The interval between $x = 0$ and $x = \Delta x$ is not a mesh. The interval between $x = a\Delta x$ and $x = \Delta x$ (the first mesh) is a times smaller than the next interval (the second mesh), etc. The value of Δx follows from the distance between the first gridpoint ($x = \Delta x$) and the last gridpoint $x = a^{ng}\Delta x$

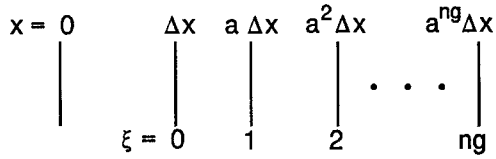

Fig. A1. Schematic presentation of gridpoints on a x-scale and ξ-scale.

$$a^{ng}\Delta x - \Delta x = H \Rightarrow \Delta x = \frac{H}{a^{ng} - 1}. \tag{A1}$$

A coordination transformation from x to ξ can now be performed to obtain for the coordinate ξ the values $0, 1, 2, \ldots, ng-1, ng$—as indicated in Fig. A1

$$\xi = \frac{\ln\left(\frac{x}{\Delta x}\right)}{\ln(a)}. \tag{A2}$$

Because an x-scale is preferred which begins at $x = 0$ for the evaporating surface in equation (A2), a shift must be made in the coordinate x with the result

$$\xi = \frac{\ln\left(x\frac{a^{ng}-1}{H} + 1\right)}{\ln(a)}, \tag{A3}$$

in which equation (A1) is used. From equation (A3) follows:

$$dx = \frac{H}{a^{ng}-1} a^{\xi} \ln(a)\, d\xi, \tag{A4}$$

which is used to transform the differential equations (6) and (12) into differential equations (22) and (23) and boundary condition (19) into equation (26).